

Time-domain violation of the optical Bloch equations for solids

R. N. Shakhmuratov* and A. Szabo

Institute for Microstructural Sciences, National Research Council of Canada, Ottawa, Ontario, Canada K1A 0R6

(Received 22 March 1993; revised manuscript received 19 May 1993)

Recent studies of the failure of the optical Bloch equations (OBE) in describing optical saturation in a solid are extended to test another aspect of the OBE, namely the time dependence of free-induction decay (FID) predicted by the SWB theorem on optical transients [Schenzle, Wong, and Brewer, *Phys. Rev. A* **22**, 635 (1980)]. This theorem states that, following an arbitrarily shaped excitation pulse of length T , the FID will vanish at time T following the end of the excitation pulse. Experiments with ruby violate SWB in that FID decay at least twice as long as the excitation pulse is observed. Numerical and analytical calculations using a Gauss-Markov model for the modified OBE show an extended FID decay, however, the theoretical decay shape does not agree with experiment. Thus as with earlier studies on saturation broadening, we find that the modified OBE provides only a qualitative description of radiation-atom interaction in a solid.

I. INTRODUCTION

Recent free-induction-decay (FID) studies have shown that the conventional optical Bloch equations (OBE) fail to describe the hole saturation behavior of the D_1 line (592.5 nm) in $\text{Pr}^{3+}:\text{LaF}_3$ (Ref. 1) and the R_1 line (693.4 nm) in $\text{Cr}^{3+}:\text{Al}_2\text{O}_3$ (ruby) (Ref. 2). Later frequency domain studies³ of ruby using hole burning have directly confirmed these observations. Another prediction of the conventional OBE is contained in the interesting theorem of Schenzle, Wong, and Brewer^{4,5}, which states that the amplitude of FID, following an arbitrary shaped resonant excitation pulse of length T , will become (and remain) identically zero after a time T following the end of the pulse. The main assumptions made are that the inhomogeneous linewidth is infinite and the sample is optically thin. For most zero-phonon lines in low-temperature crystals, the former assumption is nearly true, since the homogenous width (or alternatively, the spectral width determined by the excitation pulse length) is much less than the inhomogeneous width. For example, in ruby, the R_1 homogeneous linewidth is ~ 10 kHz compared to the inhomogeneous width of ~ 2 GHz.

The oscillatory nature of the FID predicted in Ref. 4 has been nicely verified for nuclear-magnetic resonance⁶ and for the optical case in ruby.⁷ These experiments also show, on a linear scale, that the FID becomes small at $t=T$. In this work, we report optical FID studies in ruby over a range of three orders of intensity. A large magnetic field is used, which lengthens the dephasing time and allows observation of strong FID signals for times $\sim T$ following the end of the excitation pulse.

II. EXPERIMENT

The ${}^4\text{A}_2(-3/2) \leftrightarrow \bar{\text{E}}(-1/2)$ transition in dilute (0.0034 Wt % Cr_2O_3) ruby in a field of 46.3 kG (along the c axis) was used for the experiments. The sample temperature was 1.7 K. Under these conditions the $1/e$ decay time of

echo intensity is ~ 10 μsec .⁸ A single frequency ring dye laser, stabilized to a width of 2 kHz peak to peak,² was used for resonant excitation of the R_1 line. FID was measured, using the setup described in Ref. 3, following a 5 μsec excitation pulse produced from the cw beam by an acousto-optic modulator. The FID intensity was detected by a silicon diode and the signal amplified by a low noise amplifier (Stanford Model SR560) followed by averaging with a Data Precision 6100 digital oscilloscope. The repetition rate was 25 Hz and typically 256 averages were taken. Rabi frequencies were measured by observation of the nutation period following pulse turnon.³

III. RESULT AND DISCUSSION

Figure 1 shows a FID intensity decay result for a 5- μsec pump pulse. As is evident, the FID persists well beyond 5 μsec , the time at which the SWB theorem states that the signal should become identically zero. This deviation may be linked to the failure of OBE in describing the power broadening behavior in solids.¹⁻³ Several theories (Refs. 9-12, and references therein) have been advanced to explain the latter observation with some, although not complete, success.¹² We now examine the FID time dependence of one of these models [Gauss-Markov (GM)] (Refs. 2, 11, and 13) to see if it can account for the observations. The modified optical Bloch equations (MBE) can be written as

$$\frac{d\boldsymbol{\beta}}{dt} = \hat{M}\boldsymbol{\beta} + \mathcal{L}, \quad (1)$$

$$\boldsymbol{\beta} = \begin{bmatrix} u \\ v \\ w \end{bmatrix}; \quad \mathcal{L} = 2\gamma w_{\text{eq}} \begin{bmatrix} 0 \\ 0 \\ 1 \end{bmatrix},$$

where u, v, w , are components of the Bloch vector. We assume a closed two-level system so that $2\gamma = 1/T_1$, where T_1 is the upper state lifetime. The equilibrium value w_{eq} is set to -1 . The 3×3 matrix \hat{M} can be written as

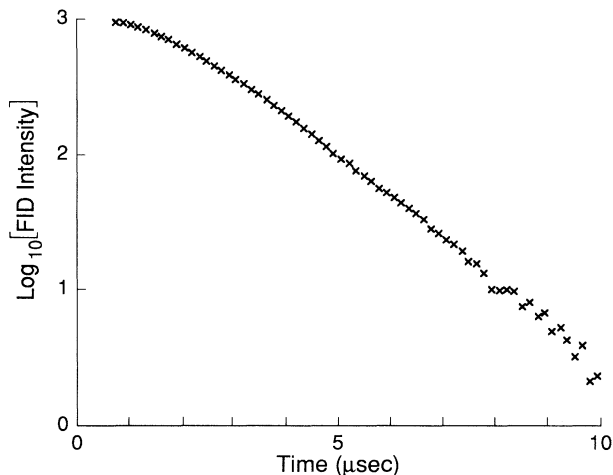


FIG. 1. Experimental free-induction decay of the ${}^4A_2(-3/2) \leftrightarrow \bar{E}(-1/2)R_1$ transition in ruby following an excitation pulse of $5\mu\text{sec}$ at a Rabi frequency of 135 kHz. Experimental conditions: 0.0034 Wt. % Cr_2O_3 , 1.6 K, 46.3 kG applied along the c axis and sample thickness = 1.6 mm.

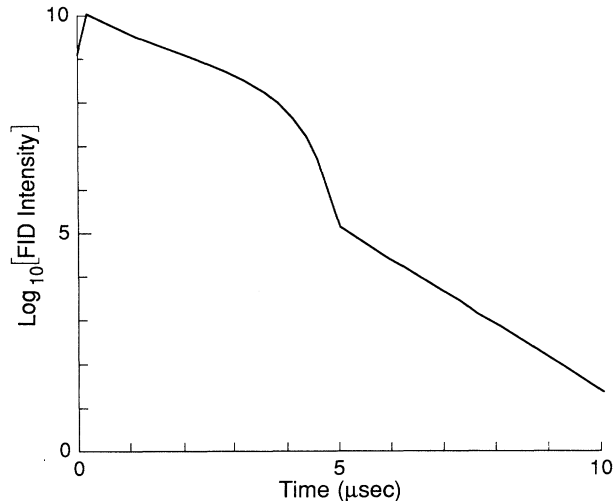


FIG. 2. Numerical calculation of free-induction decay using the Gauss-Markov model for the modified Bloch equations. The pulse parameters are pulse length = $5\mu\text{sec}$ and Rabi frequency = 135 kHz. $T_1=4200\mu\text{sec}$ and $T_2=40\mu\text{sec}$ (see text) are assumed.

$$\hat{M} = - \begin{pmatrix} \gamma & 0 & 0 \\ 0 & \gamma & 0 \\ 0 & 0 & 2\gamma \end{pmatrix} + \begin{pmatrix} 0 & -\Delta & 0 \\ \Delta & 0 & \Omega \\ 0 & \Omega & 0 \end{pmatrix} - \begin{pmatrix} \Gamma_{11} & 0 & \Gamma_{13} \\ 0 & \Gamma_{22} & \Gamma_{23} \\ 0 & 0 & 0 \end{pmatrix},$$

where the first matrix accounts for the lifetime damping, the second is the coherent driving matrix, and the third is a generalized damping matrix. For the GM dephasing model ($\gamma'\tau_c \ll 1$), the damping matrix elements are given by⁹⁻¹²

$$\begin{aligned} \Gamma_{11} &= \Gamma_{22} = \Gamma = \gamma' [1 + (\Delta\tau_c)^2] / [1 + (\Omega'\tau_c)^2], \\ \Gamma_{13} &= \gamma' \Omega \Delta \tau_c^2 / [1 + (\Omega'\tau_c)^2], \\ \Gamma_{23} &= -\gamma' \Omega \tau_c / [1 + (\Omega'\tau_c)^2], \end{aligned} \quad (2)$$

where $\gamma' = (\delta\omega)^2 \tau_c$, $\Omega' = (\Delta^2 + \Omega^2)^{1/2}$, $\Omega/2\pi$ is the Rabi frequency, $\Delta/2\pi$ is the detuning frequency, and $\delta\omega$ and τ_c are parameters of the frequency fluctuation model described in Refs. 9-12. The FID signal following the pump pulse is given by⁴

$$A(t, T) \sim \int_{-\infty}^{\infty} v(t, T, \Delta) d\Delta, \quad (3)$$

$$v(t, T, \Delta) = [u(T, \Delta) \sin \Delta t + v(T, \Delta) \cos \Delta t] e^{-(\gamma + \gamma')t},$$

where the integral assumes a flat inhomogeneous line shape, T is the pump pulse width, and t is the observation time following the end of the pulse. Numerical evaluation of the FID intensity, $A^2(t, T)$ for $T=5\mu\text{sec}$ and $\tau_c = (\gamma')^{-1} = 40\mu\text{sec}$ is shown in Fig. 2. It is clear that the SWB theorem is violated, since the FID continues well past $t=T$. However a jog appears in the decay at $t=T$, which in the Bloch limit ($\gamma' \rightarrow 0$), approaches zero as required by the SWB theorem. Because of finite computer precision however, the calculated FID intensity for

the Bloch case remains finite ~ 6 orders down from that shown in Fig. 2 at $t=T$. Evidently the modified OBE description of the FID decay does not quantitatively agree with experiment in the region $t=T$, since the latter shows only a smooth decay there. This is consistent with earlier conclusions^{2,12} that the GM model only qualitatively describes power broadening of hole burning in solids.

The validity of the SWB theorem depends on the fact that the OBE functions $u(T, \Delta)$, $v(T, \Delta)$, and $w(T, \Delta)$ do not contain singularities in the parameter Δ when T is finite. This can be shown for the OBE, with $T_1 = T_2 = \gamma^{-1}$, by a power-series expansion of the functions $\sin(\Omega'T)$, $\cos(\Omega'T)$, and $\exp(-\gamma T)$ in the u, v, w solutions. In the general case (where T_1 and T_2 are arbitrary), this is a consequence of Poincaré's theorem.^{14,5} Because the OBE are a set of first-order differential equations with coefficients linearly dependent on the parameter Δ , then the solutions are entire (integral) functions¹⁵ and are therefore analytic in Δ . When the solutions u, v, w do not contain poles in the finite complex plane Δ , then integral (3) equals zero for $t > T$.⁵ On the other hand, the MBE have coefficients nonlinearly dependent on the parameter Δ . Also these coefficients have two poles

$$\Delta = \pm i \sqrt{\Omega^2 + (1/\tau_c)^2}. \quad (4)$$

Therefore, solutions of MBE have to contain poles in the Δ complex plane and integral (3) will have a nonzero value for $t > T$. To provide this, consider part of integral (3):

$$A_v(t, T) = \int_{-\infty}^{\infty} v(T, \Delta) \cos(\Delta t) e^{-(\gamma + \gamma')t} d\Delta. \quad (5)$$

Analysis of this part will be sufficient for the proof, since if the poles exist, then they must exist in each of the func-

tions, u, v, w , because the Laplace transforms of these functions have the same denominator. Limiting the analysis to consideration of only the v contribution to the FID allows the formulation of an analytical expression without integrals. Analysis of the FID time dependence for small Rabi frequencies, for which the integrals can be approximately evaluated, is presented in the Appendix. We use the Laplace transform as in Ref. 5,

$$A_v(t, p) = \int_0^\infty A_v(t, T) e^{-pT} dT \equiv \mathcal{L}_T A_v(t, T). \quad (6)$$

The Laplace transform of the solution $v(T, \Delta)$ of Eq. (1) has the form

$$\mathcal{L}_T v(T, \Delta) = v(p, \Delta) = -\frac{p+2\gamma}{p} \frac{B}{D}, \quad (7)$$

$$B = -\Gamma_{13}\Delta + (p + \Gamma + \gamma)(\Omega - \Gamma_{23}),$$

$$D = \Delta^2(p + 2\gamma) - \Delta\Omega\Gamma_{13} + (p + 2\gamma)(p + \Gamma + \gamma)^2 + \Omega(\Omega - \Gamma_{23})(p + \Gamma + \gamma),$$

and evaluation of Eq. (6) is reduced to the integral

$$A_v(t, p) = e^{-(\gamma + \gamma')t} \int_{-\infty}^\infty v(p, \Delta) \cos(\Delta t) d\Delta. \quad (8)$$

To show the violation of the SWB theorem in the simplest way, consider the condition of

$$\Omega \gg \gamma' = \tau_c^{-1} \gg \gamma, \quad (9)$$

which allows a perturbative approach. Since Ω is the largest parameter it is convenient to introduce new variables $y = \Delta/\Omega$, $\tau_p = \Omega T$, $\tau_d = \Omega t$, $s = p/\Omega$, and the parameter $\alpha = \gamma'/\Omega$. Since $\gamma \ll \gamma'$, we simply set $\gamma = 0$. Zero-order perturbation theory on the small parameter α gives two poles for the function $v(s, y)$,

$$y_{1,2} = \pm i\sqrt{s^2 + 1} \quad (10)$$

and allows calculation of integral (8)

$$A_{v0}(\tau_d, s) = -\pi\Omega \exp[-(\alpha + \sqrt{s^2 + 1})\tau_d] / \sqrt{s^2 + 1}. \quad (11)$$

Applying the inverse Laplace transform to (11) gives the Fourier transform of the solution $v(T, \Delta)$.

$$A_{v0}(t, T) = -\pi\Omega J_0(\Omega\sqrt{T^2 - t^2}) U(T - t) e^{-\gamma' t}, \quad (12)$$

where $J_0(x)$ is a Bessel function of zero order and

$$U(x) = \begin{cases} 1 & \text{at } x > 0 \\ 0 & \text{at } x < 0 \end{cases}$$

is a unit step function. The zero-order approximation for $v(s, y)$ corresponds to neglecting dephasing in the MBE ($\gamma' = 0$). Including dephasing to first order in the parameter α changes the $y_{1,2}$ poles [Eq. (10)],

$$y_{1,2} = \pm i\sqrt{s^2 + 1} \left[1 + \frac{\alpha}{s} \right] \quad (13)$$

and gives two new poles

$$y_{3,4} = \pm i \left[1 - \frac{\alpha}{s} \right]. \quad (14)$$

The contribution of the $y_{3,4}$ poles to integral (8) and its Laplace transform gives

$$A_{v1}(t, T) = -2\pi\Omega \frac{T}{t} I_2(2\sqrt{\Omega\gamma'Tt}) \exp[-(\Omega + \gamma')t], \quad (15)$$

where $I_2(x)$ is the modified Bessel function of the second order.

For $T\gamma' \ll 1$, we can neglect changes in the poles $y_{1,2}$ and write for the Fourier transform (5) of the MBE solution $v(T, \Delta)$ as

$$A_v(t, T) = A_{v0}(t, T) + A_{v1}(t, T). \quad (16)$$

Figure 3 compares a numerically calculated curve for integral (5) with the approximate analytic solution, Eq. (16) for the case $\Omega = 135$ kHz, $T = 5\mu\text{sec}$, and $\tau_c = 300\mu\text{sec}$. The agreement is excellent and shows unambiguously that at the time $t > T$, the Fourier transform of the MBE solution exists and decays with a rate $\sim \Omega$. It confirms the initial suggestion concerning the existence of poles in the MBE solution due to the presence of poles (4) in the MBE coefficients. For the condition of (9) and $T \ll \tau_c$, these poles are reproduced in the solution and give an exponential decay of integral (5) with a rate Ω for the interval $t > T$. When the pulse width T is comparable to the correlation time, then the contribution of poles to integral (5) results in an additional dependence on T and modifies the pure exponential time dependence and rate Ω .

For small Rabi frequencies, numerical calculations show that the jog in the FID decay seen in Fig. 2 disap-

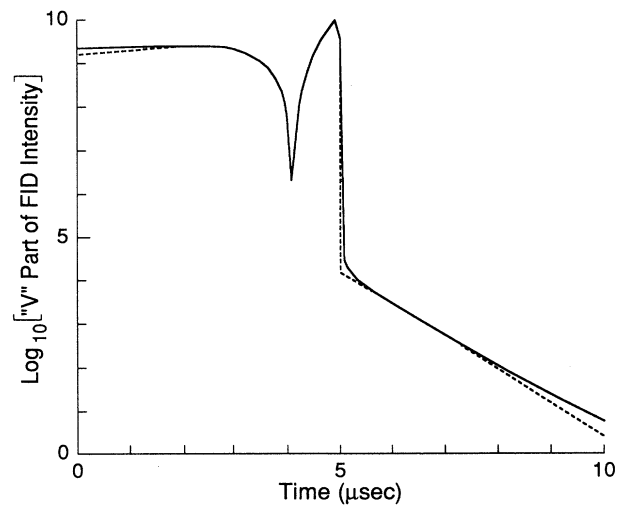


FIG. 3. Comparison of numerical calculations of $A_v^2(t, T)$ [the square of integral (5)] with analytic calculation (dotted line). Note that the dip in the curves near $t = 4\mu\text{sec}$ is due to a zero crossing. 101 points were calculated for each case causing truncation of the curves at the zero crossing.

pears and a smooth decay beyond the time $t = T$ occurs. Analysis of the GM model for this condition is discussed in the Appendix.

IV. SUMMARY AND CONCLUSIONS

We have shown experimentally that the SWB theorem is violated and that this violation may be related to the failure of the OBE in describing optical saturation in solids. Using the Gauss-Markov model of the MBE, we have shown theoretically that a long tail appears in the FID extending beyond the cutoff time predicted by the SWB theorem. This indicates a narrowing of the response spectrum of the two-level system and is consistent with the narrowing seen in the FID [(Refs. 1 and 2) and hole-burning experiments (Ref. 3)].

As noted in the Introduction, there are two assumptions that limit the validity of the SWB theorem. The effect of a finite inhomogeneous width 2δ was estimated in Ref. 5 and gives a contribution to FID at $t > T$ which is proportional to $e^{-\delta t}$ and is far below the observations for ruby. Another possible explanation of the observations is that our sample is not optically thin. The unsaturated transmission was measured to be $\sim 20\%$. A complete description of the FID requires a solution of the Maxwell-Bloch equations. These equations are nonlinear and hence the SWB theorem is not valid. This can be shown qualitatively by considering excitation of two optically thin samples in series. The total emission time following the second slice will be $4T$, violating the SWB theorem. However, one might expect a jog to appear in the FID decay at time T , similar to that in Fig. 2 as the sample thickness decreases. This could be experimentally studied by moving the excitation frequency toward the edge of the inhomogeneous line. Further experimental and theoretical investigations are planned to test the various modified OBE predictions of the FID decay shape.

APPENDIX

We examine the conditions for which the contribution to the FID decay due to the OBE modification dominates over the unmodified contribution. This occurs when the Rabi frequency is small and the dephasing is slow ($\gamma'T < \Omega T < 1$). In this case, an approximate analytical expression for the FID [Eq. (3)] may be derived. We write for the FID amplitude

$$A(t, T) = A_0(t, T) + A_1(t, T), \quad (\text{A1})$$

where $A_0(t, T)$ is the contribution due to the standard OBE and $A_1(t, T)$ is the modification due to the GM model. Using the same steps and approximations as in Sec. III we obtain

$$A_0(t, T) = \pi\Omega^2 e^{-\gamma't} U(T-t) \times \int_t^T \left(\frac{x-t}{x+t} \right)^{1/2} J_1(\Omega\sqrt{x^2-t^2}) e^{-\gamma'x} dx,$$

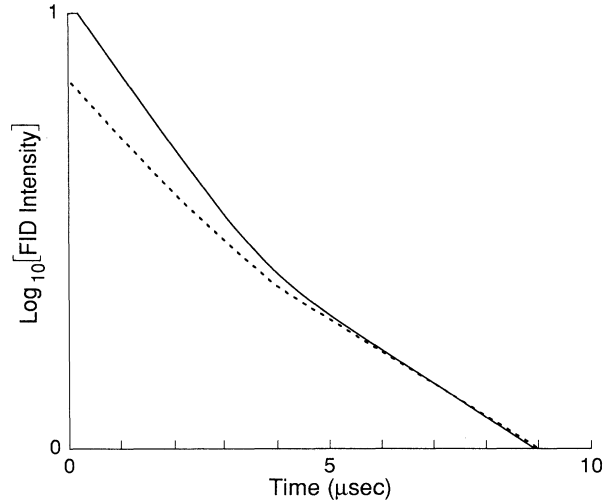


FIG. 4. Comparison of numerically calculated free-induction decay with approximate analytic result [dotted line, the square of Eq. (17)] for the Gauss-Markov model of modified optical Bloch equations; $\Omega = 10$ kHz, $T = 5$ μ sec, $\tau_c = T_2 = 40$ μ sec, and $T_1 = 4200$ μ sec. For these conditions, the GM contribution to the decay dominates and a smooth decay occurs in the region $t = T$ as discussed in the text.

$$A_1(t, T) = 2\pi\Omega\gamma'T \left[\frac{1}{z} I_1(z) - \frac{4\Omega T}{z^2} I_2(z) + 8 \frac{(\Omega T)^2}{z^3} I_3(z) \right] e^{-(\Omega + \gamma')t},$$

where $z = 2\sqrt{\Omega\gamma'tT}$ and $J_n(x), I_n(x)$ are Bessel and modified Bessel functions of order n , respectively. For the condition

$$1 > \gamma'T \left[1 - \Omega T + \frac{1}{3}(\Omega T)^2 \right] > \frac{(\Omega T)^2}{4}, \quad (\text{A2})$$

the FID contribution due to $A_1(t, T)$ dominates that due to $A_0(t, T)$. A comparison of a numerical calculation² with the analytic expression $A^2(t, T)$, obtained from Eq. (A1) for the parameters $\Omega = 10$ kHz, $T = 5$ μ sec, $\tau_c = (\gamma')^{-1} = 40$ μ sec [satisfying condition (A2)], is shown in Fig. 4. An approximate expression for $A_0(t, T)$ was used.

$$A_0(t, T) = \frac{1}{2}\pi\Omega(\Omega/\gamma')^2 e^{-2\gamma't} \times \{ 1 - [1 + (T-t)\gamma'] e^{-\gamma'(T-t)} \} U(T-t),$$

obtained by using the first term, $x/2$ in the power-series expansion of $J_1(x)$. It is evident that the predominance of $A_1(t, T)$ over $A_0(t, T)$ leads to a smooth decay of the FID in the region $t = T$.

- *Permanent address: Kazan Physical Technical Institute of Russian Academy of Sciences, Kazan 420029, Russia.
- ¹R. G. DeVoe and R. G. Brewer, *Phys. Rev. Lett.* **50**, 1269 (1983).
- ²A. Szabo and T. Muramoto, *Phys. Rev. A* **39**, 3992 (1989).
- ³A. Szabo and R. Kaarli, *Phys. Rev. B* **44**, 12 307 (1991).
- ⁴A. Schenzle, N. C. Wong, and R. G. Brewer, *Phys. Rev. A* **21**, 887 (1980).
- ⁵A. Schenzle, N. C. Wong, and R. G. Brewer, *Phys. Rev. A* **22**, 635 (1980).
- ⁶M. Kunitomo, T. Endo, S. Nakanishi, and T. Hashi, *Phys. Lett.* **80A**, 84 (1980).
- ⁷T. Endo, S. Nakanishi, T. Muramoto, and T. Hashi, *Opt. Commun.* **37**, 369 (1981).
- ⁸A. Szabo (unpublished).
- ⁹A. Schenzle, M. Mitsunaga, R. G. DeVoe, and R. G. Brewer, *Phys. Rev. A* **30**, 325 (1984).
- ¹⁰M. Yamanoi and J. H. Eberly, *Phys. Rev. Lett.* **52**, 1353 (1984); *J. Opt. Soc. Am. B* **1**, 751 (1984).
- ¹¹P. R. Berman and R. G. Brewer, *Phys. Rev. A* **32**, 2784 (1985).
- ¹²P. R. Berman, *J. Opt. Soc. Am. B* **3**, 564 (1986); **3**, 572 (1986).
- ¹³A. Szabo and T. Muramoto, *Phys. Rev. A* **37**, 4040 (1988).
- ¹⁴J. H. Poincare, *Les Methodes Nouvelles de la Mecanique Celeste* (Dover, New York, 1957), Vol. 1, p. 48.
- ¹⁵G. A. Korn and T. M. Korn, *Mathematical Handbook for Scientists and Engineers* (McGraw-Hill, New York, 1961), p.195.